

Radar and Navigation

UDC 621.391

Original article

<https://doi.org/10.32603/1993-8985-2022-25-4-63-71>

Estimating Disturbance Torque Effects on the Stability and Control Performance of Two-Axis Gimbal Systems

Ngoc Hung Nguyen , Van Phan Do, Hoa Tien Vu

Le Quy Don Technical University, Hanoi, Vietnam

 hungnn@lqdtu.edu.vn

Abstract

Introduction. Two-axis gimbal systems are applied for stabilizing and controlling the line of sight (LOS) of an optical or imaging system mounted on a moving vehicle. Gimbal systems are intended to isolate various disturbance torques and control the LOS toward the direction of a target. Two-axis gimbals can be of two main types, namely Yaw-Pitch and Swing-Roll type. In this article, we focus on investigating mathematical models of two-axis gimbals, which describe the impact of cross-disturbance torques on their stability and control performance. Simulations were conducted to compare advantages and disadvantages of the two types of two-axis gimbals.

Aim. To study mathematical models describing the impact of cross-disturbance torques on the stability and control performance of two-axis gimbals.

Materials and methods. Mathematical models of two-axis gimbal systems were synthesized by the Lagrange method. The operation of two-axis gimbal systems was simulated in the Matlab-Simulink environment.

Results. Mathematical models and structural diagrams of the synthesized Yaw-Pitch and Swing-Roll gimbals were obtained. The conducted simulations of typical cases revealed different cross-disturbance effects.

Conclusion. Motion equations for Swing-Roll and Yaw-Pitch gimbals were derived using similar methodology. The impact of cross-disturbance torques on gimbal systems was evaluated. The obtained results form a basis for selecting an optimal structure of tracking systems meeting the desired characteristics.

Keywords: two-axis gimbal, disturbance torque, inertially-stabilized platform

For citation: Ngoc Hung Nguyen, Van Phan Do, Hoa Tien Vu. Estimating Disturbance Torque Effects on the Stability and Control Performance of Two-Axis Gimbal Systems. Journal of the Russian Universities. Radioelectronics. 2022, vol. 25, no. 4, pp. 63–71. doi: 10.32603/1993-8985-2022-25-4-63-71

Conflict of interest. The authors declare no conflicts of interest.

Submitted 02.04.2022; accepted 26.05.2022; published online 28.09.2022



Introduction. Stabilization and line-of-sight control systems installed in optical devices, such as cameras or optical sensors, have found wide application [1]. These systems comprise a gimbal, an inertial angular rate and angle sensor, and a control subsystem. Accordingly, the selection of an appropriate gimbal architecture for specific application domains has a significant influence on the system's ability to stabilize and control the line of sight (LOS). In practice, three types of gimbal systems are commonly used: three-axis gimbals [2], Yaw-Pitch two-axis gimbals [3], and Swing-Roll two-axis gimbals [4]. Although exhibiting the highest stability [5], three-axis gimbals are complex in structure and are applicable in systems covering a relatively large space. Therefore, two-axis gimbals are used in devices having restrictions on mass and size, e. g., an imaging gimballed seeker [6, 7]. Compared to Swing-Roll gimbals, Yaw-Pitch two-axis gimbals are controlled by two independent channels according to the cartesian coordinate system, which fact determines their popularity [8–11]. This is consistent with the process of tracking an object along two axes on a camera image. Swing-Roll gimbals control the polar coordinate system, therefore requiring conversion of the camera's coordinate system into the gimbal's coordinate system [6]. However, according to [4], Swing-Roll systems outperform Yaw-Pitch systems in terms of expanded field of view. The selection of an appropriate gimbal structure for particular purposes depends on its ability to separate the carrier's movements from the optical axis. Therefore, research into the impact of disturbance torques on the stability and control performance of various two-axis gimbal systems presents a relevant task.

In this paper, we investigate the applicability of various gimbal types for space-limited seeker systems. In this regard, we focus on comparing the impact of disturbance torques on the above-mentioned two-axis gimbal types.

The paper is organized as follows. First, we construct mathematical models of two-axis gimbal systems. Secondly, a structural analysis of the gimbal systems under study is carried out. Thirdly, the simulation, evaluation, and comparison results of

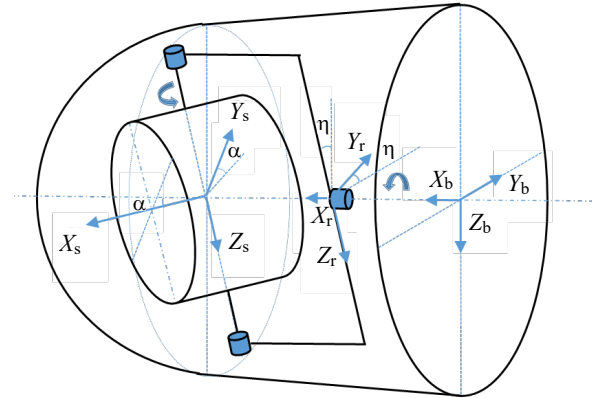


Fig. 1. Structure of Swing-Roll gimbal

disturbance torque effects on the stability and control performance of the two-axis gimbals under study are presented. Finally, the conclusions are drawn.

Mathematical models of two-axis gimbals.

Yaw-Pitch two-axis gimbal. The architecture of a Yaw-Pitch 2-axis gimbal is presented in Fig. 1, which shows two axes of rotation in elevation and azimuth channels. The azimuth channel (Yaw) is a channel that rotates around the Z_b axis of the connected coordinate system with a rotation angle β. The elevation channel (Pitch) is a channel rotated around the Y_h axis of the seeker's coordinate system with a rotation angle ε. The designations used in Fig. 1 are as follows:

X_b, Y_b, Z_b – body coordinate system (Body – B);

X_h, Y_h, Z_h – coordinate system of the homing head (Head – H);

X'_h, Y_h, Z_b – coordinate system of the azimuth frame (Yaw – Y).

Accordingly, the directional cosine matrix converted from the body coordinate system to the azimuth frame coordinate system is C_b^y , while that converted from the azimuth frame coordinate system to the homing head coordinate system is C_y^h :

$$C_b^y = \begin{bmatrix} \cos \beta & \sin \beta & 0 \\ -\sin \beta & \cos \beta & 0 \\ 0 & 0 & 1 \end{bmatrix};$$

$$C_y^h = \begin{bmatrix} \cos \varepsilon & 0 & -\sin \varepsilon \\ 0 & 1 & 0 \\ \sin \varepsilon & 0 & \cos \varepsilon \end{bmatrix}. \quad (1)$$

Let the inertial rotational rate of the coordinate systems along its axes be:

$$\omega_{B/I}^B = [P_b \quad Q_b \quad R_b]^T; \quad \omega_{H/I}^H = [p_h \quad q_h \quad r_h]^T$$

$$\text{and } \omega_{Y/I}^Y = [p_y \quad q_y \quad r_y]^T.$$

Then, the speed vector of inertia angle that is represented in the azimuth frame will take the form:

$$\omega_{Y/I}^Y = C_b^y \omega_{B/I}^B + [0 \quad 0 \quad \dot{\beta}]^T. \quad (2)$$

And the speed vector of inertia angle that is represented in the elevation frame will be:

$$\omega_{H/I}^H = C_y^h \omega_{Y/I}^Y + [0 \quad \varepsilon \quad 0]^T. \quad (3)$$

Let the matrix of the inertia moment of the elevation frame take the form, respectively:

$$J_Y = \begin{bmatrix} J_x^y & J_{xy}^y & J_{xz}^y \\ J_{xy}^y & J_y^y & J_{yz}^y \\ J_{xz}^y & J_{yz}^y & J_z^y \end{bmatrix};$$

$$J_H = \begin{bmatrix} J_x^h & J_{xy}^h & J_{xz}^h \\ J_{xy}^h & J_y^h & J_{yz}^h \\ J_{xz}^h & J_{yz}^h & J_z^h \end{bmatrix}.$$

The angular momentum is given by the expression $H = J\omega$. Then, the equation for a rotation moment with respect to the elevation frame will take the form

$$\Gamma^P = \frac{\partial}{\partial t} H^P + \omega_{Y/I}^Y H^P. \quad (4)$$

By substituting (1), (2) and (3) into (4) and assuming that the gimbal's texture is rigid, the following expression can be obtained after a few transformations

$$J_y^h \dot{q}_h = T_y + (J_z^h - J_x^h) p_h r_h + J_{xz}^h (p_h^2 - r_h^2) - J_{yz}^h (\dot{r}_h - p_h q_h) - J_{xy}^h (\dot{p}_h - q_h r_h), \quad (5)$$

where T_y is the sum of torques acting on the elevation frame system. In the absence of other disturbance torques (such as friction), this is the torque produced by the motor. On the right side of expression (5), the components containing the moment of inertia describe cross-channel connections in the presence of movement along other axes. Therefore, expression (5) can be considered as a complete form modeling the elevation frame dynamics. When substituting (3) into expression (5), the disturbance components arising due to cross disturbance are calculated by the formula:

$$T_D = T_B + T_C, \quad (6)$$

where

$$T_B = -\left(J_{yz}^h \sin \varepsilon + J_{xy}^h \cos \varepsilon\right) (\dot{p}_y + q_y r_y) + \left(J_{yz}^h \cos \varepsilon + J_{xy}^h \sin \varepsilon\right) p_y q_y + \left[\left(J_z^h - J_x^h\right) \cos(2\varepsilon) - 2J_{xz}^h \sin(2\varepsilon)\right] p_y r_y + \frac{1}{2} \left[\left(J_z^h - J_x^h\right) \sin(2\varepsilon) - 2J_{xz}^h \cos(2\varepsilon)\right] p_y^2; \quad (7)$$

$$T_C = \left(J_{xy}^h \sin \varepsilon + J_{yz}^h \cos \varepsilon\right) \dot{r}_y + \frac{1}{2} \left[\left(J_z^h - J_x^h\right) \sin(2\varepsilon) - 2J_{xz}^h \cos(2\varepsilon)\right] r_y^2. \quad (8)$$

This finding shows that cross-disturbance components persist even in the absence of the system's movement. Hence, when $P_b = 0$; $Q_b = 0$; $R_b = 0$, then $T_B = 0$ according to (2). However, due to $r_y \neq 0$; therefore, $T_C \neq 0$. It can be seen from T_B and T_C that, provided that the gimbal system ensures absolute symmetry (mean that $J_{xy}^h = J_{yz}^h = J_{xz}^h$) and $J_x^h = J_z^h$, then there will be no cross-disturbance components $T_D = 0$. However, the absence of any cross disturbance is almost impossible to observe in practice, including in two-axis gimbal systems. Consequently, these components should always be calculated in order for their negative impact to be eliminated.

The formation of a dynamic model for the azimuth channel (Yaw) is preformed similarly to the approach described above. According to [3],

$$J^y \dot{r}_y = T_z + T_{d1} + T_{d2} + T_{d3}, \quad (9)$$

where

$$J^y = J_z^y + J_x^h \sin^2 \varepsilon + J_z^h \cos^2 \varepsilon - J_{xz}^h \sin^2 (2\varepsilon); \quad (10)$$

$$T_{d1} = \left[J_x^y + J_x^h \cos^2 \varepsilon + J_z^h \sin^2 \varepsilon - J_{xz}^h \sin 2\varepsilon \right] p_y q_y; \quad (11)$$

$$T_{d2} = - \left[J_{xz}^y + (J_z^h - J_z^h) \sin \varepsilon \cos \varepsilon + J_{xz}^y \cos (2\varepsilon) \right] (\dot{p}_y - q_y r_y) - \left[J_{yz}^y + J_{yz}^h \cos \varepsilon - J_{xy}^h \sin \varepsilon \right] (\dot{q}_y - p_y r_y) - \left[J_{xy}^y + J_{xy}^h \cos \varepsilon + J_{yz}^h \sin \varepsilon \right] (p_y^2 - q_y^2); \quad (12)$$

and

$$T_{d3} = \ddot{\varepsilon} \left[J_{xz}^h \sin \varepsilon + J_{yz}^h \cos \varepsilon \right] + \dot{\varepsilon} \left[(J_x^h - J_z^h) (p_y \cos 2\varepsilon - r_y \sin 2\varepsilon) \times \right. \\ \left. \times 2 J_{xz}^h (p_y \sin 2\varepsilon - r_y \cos 2\varepsilon) \right] + \dot{\varepsilon} \left[(J_{yz}^h \sin \varepsilon - J_{xy}^h \cos \varepsilon) (q_h + q_y) - J_x^h p_y \right]. \quad (13)$$

Equation (9) is a differential form of the angular rate along the z -axis of the azimuth frame for a 2-axis gimbal, where T_z is the total number of the moments acting on this shaft. The components T_{d1}, T_{d2}, T_{d3} are disturbances caused by the cross-channel relationship affecting the gimbal system.

It can be seen that J^y calculated by expression (10) is the total moment of inertia along the z -axis, varying in time and depending on the rotation angle of the elevation channel of a two-axis gimbal system. Components T_{d1}, T_{d2}, T_{d3} are disturbances caused by the cross-channel relationship. When no such a relationship is observed, the moment of inertia $J_{xz}^h = 0$. In order for J^y to be time-invariant, the condition $J_x^h = J_z^h$ must be satisfied. However, this is rarely achieved, since a gimbal is frequently equipped with a camera in practice. Therefore, a two-axis gimbal is inevitably a non-linear system.

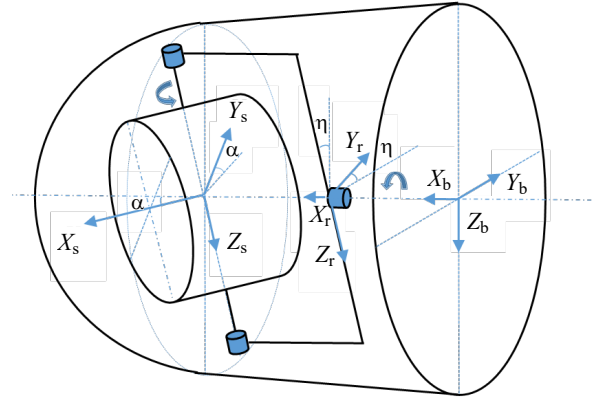


Fig. 2. Structure of Swing-Roll gimbal

The components T_{d1}, T_{d2}, T_{d3} are disturbances generated by the cross-channel relationship. When the elevation angle is fixed, only two components – T_{d1}, T_{d2} , – are present, which can be considered as stiffness coefficients in the motion equation. When $\varepsilon \neq 0$, a moment action T_{d3} can be added, which is considered as the object's deformation component.

Equations (11)–(13) show that, even when the design of a gimbal system satisfies $J_{xy}^h = J_{yz}^h = J_{xz}^h = 0$, the disturbance components generated by the cross-channel relationships still exist due to $J_x^h \neq J_z^h$. Therefore, these disturbance components can hardly be eliminated by perfecting the mechanical structure design.

Swing-Roll two-axis gimbal. Fig. 2 presents a two-axis Swing-Roll gimbal system, in which the Roll channel is a channel that rotates around the axis X_r of the Roll frame with a rotation angle η . The Swing channel is a channel that rotates around the axis X_s of the Swing frame with a rotation angle α .

A mathematical model for a Swing-Roll gimbal system can be constructed similarly to that of a Yaw-Pitch gimbal system.

The coordinate systems in Fig. 2 include:

X_r, Y_r and Z_r – the coordinate system of the Roll frame (R);

X_s, Y_s and Z_s – the coordinate system of the Swing frame (S).

The directional cosine matrix converted from

the associated coordinate system to the coordinate system of the Roll frame is C_b^r , while the directional cosine matrix converted from the coordinate system of the Roll frame to the coordinate system of the Swing frame is C_r^s :

$$C_b^r = \begin{bmatrix} 1 & 0 & 0 \\ 0 & \cos \eta & \sin \eta \\ 0 & -\sin \eta & \cos \eta \end{bmatrix}; \quad (14)$$

$$C_r^s = \begin{bmatrix} \cos \alpha & \sin \alpha & 0 \\ -\sin \alpha & \cos \alpha & 0 \\ 0 & 0 & 1 \end{bmatrix}.$$

Let the inertial rotational rate of the coordinate systems along its axes be: $\omega_{S/I}^S = [p_s \quad q_b \quad r_b]^T$;

$$\omega_{R/I}^R = [p_r \quad q_r \quad r_r]^T.$$

In this case, the vectors of the angular rate of inertia for the Roll frame and the Swing frame, respectively, take the form:

$$\omega_{R/I}^R = C_b^r \omega_{B/I}^B + [\dot{\eta} \quad 0 \quad 0]^T; \quad (15)$$

$$\omega_{S/I}^S = C_r^s \omega_{R/I}^R + [0 \quad 0 \quad \dot{\alpha}]^T. \quad (16)$$

By designating the matrices of inertia moments for the Roll frame and the Swing frame as J_R and J_S , respectively, the following is obtained:

$$J_R = \begin{bmatrix} J_x^r & J_{xy}^r & J_{xz}^r \\ J_{xy}^r & J_y^r & J_{yz}^r \\ J_{xz}^r & J_{yz}^r & J_z^r \end{bmatrix};$$

$$J_S = \begin{bmatrix} J_x^s & J_{xy}^s & J_{xz}^s \\ J_{xy}^s & J_y^s & J_{yz}^s \\ J_{xz}^s & J_{yz}^s & J_z^s \end{bmatrix}.$$

By substituting (14), (15) and (16) into (4), the motion equation of Swing frame is:

$$J_z^s \dot{r}_s = T_z + T_D^s;$$

$$T_D^s = (J_x^s - J_y^s) p_s q_s + J_{xy}^s (p_s^2 - q_s^2) - J_{xz}^s (\dot{p}_s - p_s r_s) - J_{yz}^s (\dot{q}_s - q_s r_s). \quad (17)$$

Expressions (5) and (17) show that the impact of disturbances caused by the cross-channel relationship for the two types of gimbal systems under study has similar characteristics. However, the disturbances arising from each rotation along the axes is different. Therefore, in order to minimize the impact of these disturbances, an optimal gimbal should be selected based on the motion properties of each carrier.

The dynamic equation of motion for the Roll channel is described as follows:

$$J^r \dot{p}_r = T_x + T_1 + T_2 + T_3 + T_4 + T_5 + T_6, \quad (18)$$

where

$$J^r = J_x^r + J_x^s \cos^2 \alpha + J_x^s \sin^2 \alpha + J_{xy}^s \sin(2\alpha); \quad (19)$$

$$T_1 = - \left[J_{xy}^r + (J_y^s - J_x^s) \sin \alpha \cos \alpha + J_{xy}^s \cos(2\alpha) \right] (\dot{q}_r - p_s r_s); \quad (20)$$

$$T_2 = - \left(J_{xz}^r + J_{xz}^s \cos \alpha + J_{yz}^s \sin \alpha \right) \times (\dot{r}_r + p_r q_r); \quad (21)$$

$$T_3 = - \left(J_{yz}^r + J_{xz}^s \sin \alpha \cos \alpha + J_{yz}^s \cos \alpha \right) \times (q_r^2 + r_r^2); \quad (22)$$

$$T_4 = \left[\left(J_y^r + J_x^s \sin^2 \alpha - J_{xy}^s \sin(2\alpha) + J_y^s \cos^2 \alpha \right) - \left(J_z^r + J_z^s \right) \right] q_r r_r; \quad (23)$$

$$T_5 = - \left(J_{xz}^s \cos \alpha + J_{yz}^s \sin \alpha \right) \ddot{\alpha}; \quad (24)$$

$$T_6 = - \left[\left(J_{xz}^s \cos \alpha + J_{yz}^s \sin \alpha \right) + \left(-J_x^s \sin(2\alpha) + 2J_{xy}^s \cos(2\alpha) + J_y^s \sin(2\alpha) \right) p_r \right] \dot{\alpha} - \left[\left(J_y^s - J_x^s \right) \cos(2\alpha) - 2J_{yz}^s \sin(2\alpha) + J_z^s \right] q_r \dot{\alpha}. \quad (25)$$

The above equations provide a systematic understanding of the nature of the Roll channel movement in differential forms with respect to the angular rate around the axis X , where T_x is the total moments acting on this axis, including those

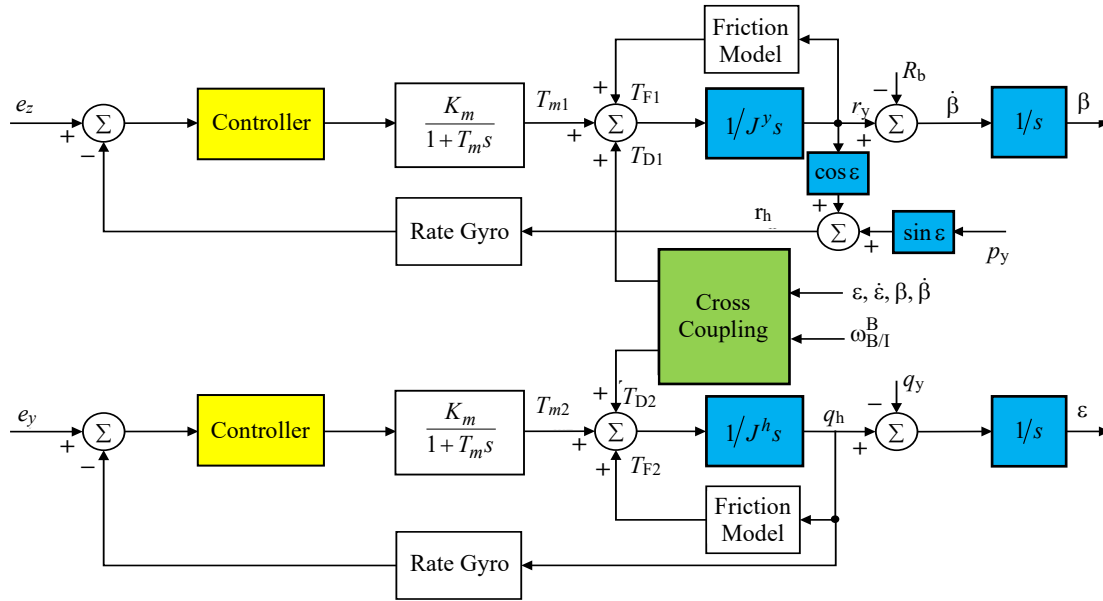


Fig. 3. Structure of control system using a Yaw-Pitch gimbal

generated by both the motor and friction. Equations (20)–(25) show the disturbance torques caused by the cross-channel relationship. In the absence of movement along the Swing channel, $\dot{\alpha} = 0$ and, hence, $T_5 = T_6 = 0$. In this case, the components $T_1 \div T_4$ are considered as moments caused by the cross-disturbance of a rigid body. However, in the presence of movement along the Swing channel, moments T_5, T_6 are understood as those generated by the object deformation.

Synthesis of a block diagram for a two-axis gimbal system. Fig. 3 presents a block diagram outlining the operation of a control system that stabilizes the line of sight using a two-axis Yaw-Pitch gimbal. This diagram was developed based on equations (2)–(13) and the model of cross-disturbance effects described by (6) and (9). In the diagram, a DC motor is used with a reduced transfer function in the form $\frac{K_m}{1 + T_m s}$ [12]. The struc-

ture diagram for a Swing-Roll two-axis gimbal system is built solely on the basis of equations (15)–(25). The controller is selected from an array of the known control laws, depending on the requirements of accuracy, noise damping, robustness, and simplicity of implementation. Since this work is aimed at investigating the impact of cross-disturbance effects and object movement on the stability of the line of sight, a canonical PI controller [7, 8] was selected for simulations. A study of

controllers in terms of damping noise and ensuring accuracy will be presented in another paper.

Disturbance torques that affect the performance of two-axis stabilization systems include not only effects caused by the cross-channel relationship due to imbalance, but also those caused by the drive system friction [13, 14]. Disturbance friction torques acting on the two gimbal systems are rather similar, since both of them have two axes. In addition, the effect of friction can be reduced by selecting a gimbal system manufactured according to a qualitative technology and a motor having a sufficient torque. Therefore, in this paper, the moment of friction is not considered.

Accordingly, this section will compare disturbance effects on the two-axis gimbal systems under study to provide a basis for selecting and synthesizing a line-of-sight stabilization control system for specific application domains.

In order to ensure the convergence of theoretical and actual data, all parameters were pre-calculated and re-calibrated using a parameter identification method [15]. The symbols e_y and e_z denote the angular error between the line of sight and the axis of the homing head issued by the target image tracking system (optical or radar).

Simulation results.

Input data. The input data is presented in Table 1, where K_p and K_i are obtained from the PID tuning tool of the MatLab software.

Tab. 1. Parameter values of the gimbal system

Nodes	Parameter
Motor	$\frac{K_m}{1+T_m s}$; $K_m = 0.85$; $T_m = 0.0135[s]$
Angular rate sensor	$\frac{\omega_g^2}{s^2 + 2\xi\omega_g s + \omega_g^2}$; $\xi = 0.7$; $\omega_g = 100 \text{ Hz}$
Moment of inertia	$J_Y = \begin{bmatrix} 0.0054 & -0.003 & -0.002 \\ -0.003 & 0.0025 & -0.003 \\ -0.002 & 0.003 & 0.0032 \end{bmatrix}$
	$J_H = \begin{bmatrix} 0.0024 & -0.001 & -0.0005 \\ -0.001 & 0.0012 & -0.001 \\ -0.0005 & 0.001 & 0.0018 \end{bmatrix}$
Controller	$K_p + \frac{K_i}{s}$

Simulation options. The simulation options are presented in Tab. 2, where P_b , Q_b and R_b are the angular rates of x -axis, y -axis, and z -axis of the body, respectively.

Tab. 2. Simulation scenes

Scene	Angular rate, deg/s		
	P_b	Q_b	R_b
1	0	0	0
2	0	1.5	12
3	0	12	1.5
4	180	1.5	1.5

Results. The simulation results for the Yaw-Pitch gimbal system under study are presented in Fig. 4, where Fig. 4, *a* shows the simulation results according to scenes 1–4 (S1 to S4) based on the input data (Tab. 1) for the Azimuth channel. Fig. 4, *b* displays the simulation results according to scenes 1–4 based on the input data (Tab. 1) for the Elevation channel.

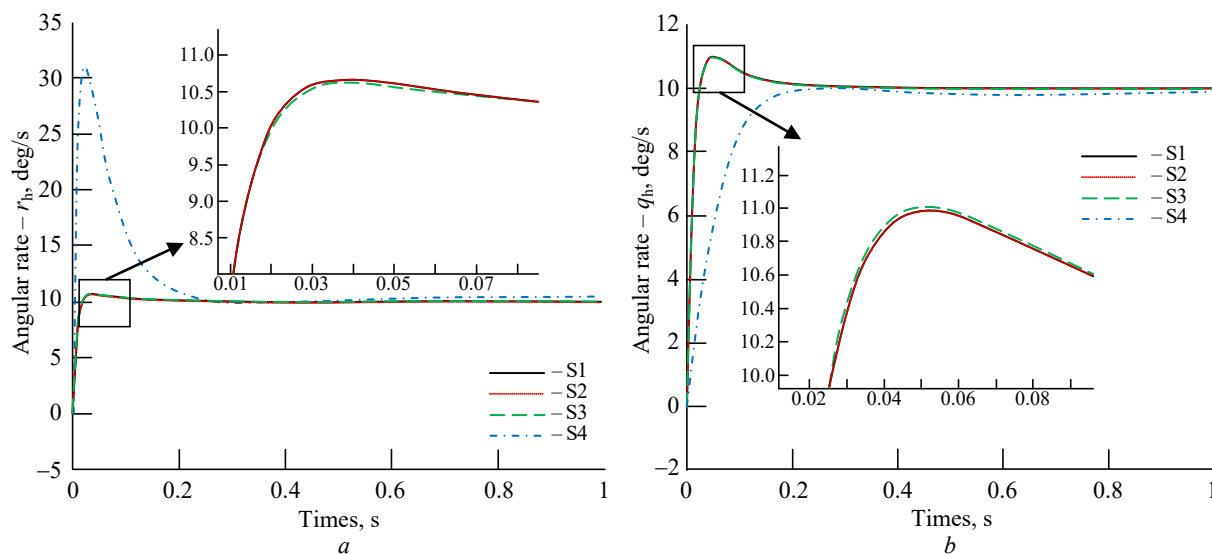


Fig. 4. Simulation results for the Yaw-Pitch gimbal system: *a* – azimuth channel; *b* – elevation channel

Simulation results for the Swing-Roll gimbal system are presented in Fig. 5, where Fig. 5, *a* shows the simulation results according to scenes 1–4 (S1 to S4) based on the input data (Tab. 1) for the Swing channel. Fig. 5, *b* displays the simulation results according to scenes 1–4 based on the input data (Tab. 1) for the Roll channel.

Discussion. The conducted simulations for the analyzed four cases of the carrier's rotation, which affects the stability and control performance of the two types of two-axis gimbals under study, have revealed the following.

1. Under the conditions where the carrier only maneuvers along the direction of motion without rotating around the x -axis (option 1–3), both gimbal systems produce relatively good results.

2. Under the conditions of the fourth scene, when the carrier rotates around the x -axis, the Yaw-Pitch gimbal system underperforms greatly both in terms of overshoot, settling time, and steady-state error. These findings are consistent with the dynamics of the two types of gimbal systems synthesized using the mathematical models presented above.

3. When using a Yaw-Pitch gimbal system, the selection of some seeker types will require installation of an additional axis system to stabilize the body's rotation. This, as a result, will produce a three-axis gimbal system with a more complicated mechanical structure.

The conducted analysis shows that Swing-Roll gimbal systems outperform Yaw-Pitch gimbal systems in terms of their ability to expand the field of

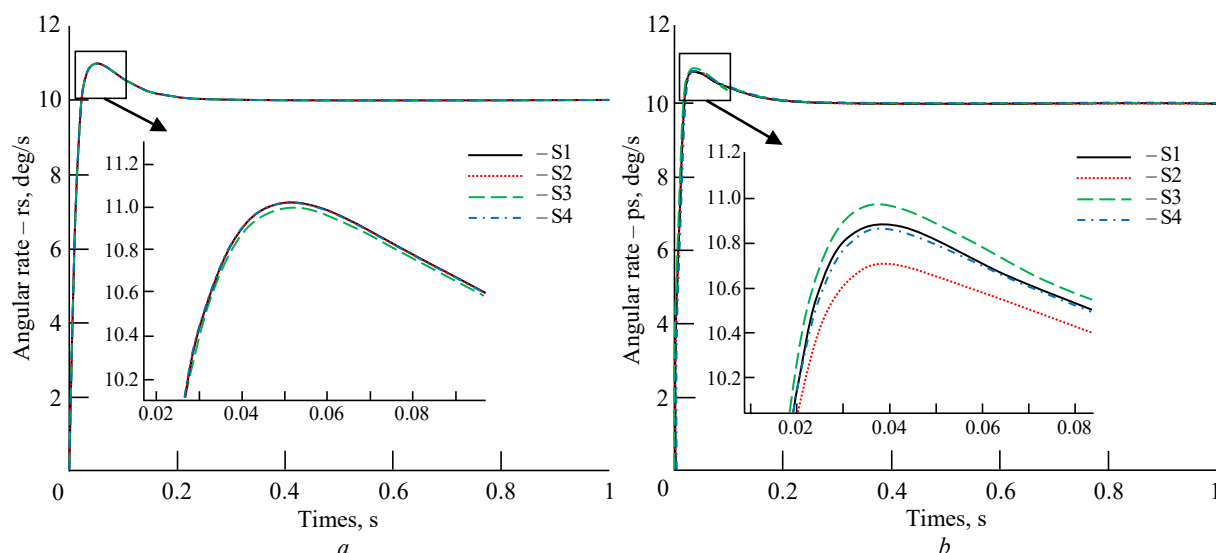


Fig. 5. Simulation results for the Swing-Roll gimbal system: *a* – Swing channel; *b* – Roll channel

view by eliminating negative cross-disturbance effects. However, Swing-Roll systems have the disadvantage of large mechanical dimensions due to the need to use a slip ring for the Roll axis. This increase the amount of calculations necessary to transform the coordinate system.

Conclusion. In this paper, we analyze solutions to the problem of stabilizing and controlling the trajectory of a homing head. Mathematical

models were synthesized for two standard two-axis gimbal systems – Yaw-Pitch and Swing-Roll – to investigate cross disturbance effects acting on these systems. Several typical cases were simulated for evaluating and comparing disturbance torque effects on the stability and control performance of various gimbal systems. The obtained results may serve as a basis for selecting a suitable gimbal system for specific practical purposes.

References

- Hilkert J. Inertially Stabilized Platform Technology Concepts and Principles. IEEE Control Systems Magazine. 2008, vol. 28, no. 1, pp. 26–46. doi: 10.1109/MCS.2007.910256
- Altan A., Hacıoğlu R. Modeling of Three-Axis Gimbal System on Unmanned Air Vehicle (UAV) under External Disturbances. 25th Signal Processing and Communications Applications Conf. (SIU), Antalya, Turkey, 15–18 May 2017. doi: 10.1109/SIU.2017.7960196
- Ekstrand B. Equations of Motion for a Two-Axes Gimbal System. IEEE Transactions on Aerospace and Electronic Systems. 2001, vol. 37, no. 3, pp. 1083–1091. doi: 10.1109/7.953259
- Bai Y., Liu B., Guo L. Design and Analysis of Roll-Swing Imaging Seeker Scan Scheme. 2nd Intern. Conf. on Industrial Mechatronics and Automation, Wuhan, China, 30–31 May 2010. doi: 10.1109/ICINDMA.2010.5538080
- Fang J., Yin R., Lei X. An Adaptive Decoupling Control for Three-Axis Gyro Stabilized Platform Based on Neural Networks. Mechatronics. 2015, vol. 27, pp. 38–46. doi: 10.1016/j.mechatronics.2015.02.002
- Jiang H., Jia H., Wei Q. Analysis of Zenith Pass Problem and Tracking Strategy Design for Roll-Pitch Seeker. Aerospace Science and Technology. 2012, vol. 23, no. 1, pp. 345–351. doi: 10.1016/j.ast.2011.08.011
- Li S., Zhong M., Zhao Y. Estimation and Compensation of Unknown Disturbance in Three-Axis Gyro-Stabilized Camera Mount. Transactions of the Institute of Measurement and Control. 2015, vol. 37, no. 6, pp. 732–745. doi: 10.1177/0142331214544498
- Abdo M. M., Vali A. R., Toloei A. R., Arvan M. R. Stabilization Loop of a Two Axes Gimbal System Using Self-Tuning PID Type Fuzzy Controller. ISA transactions. 2014, vol. 53, no. 2, pp. 591–602. doi: 10.1016/j.isatra.2013.12.008
- Bharali J., Buragohain M. Design and Performance Analysis of Fuzzy LQR; fuzzy PID and LQR Controller For Active Suspension System Using 3 Degree of Freedom Quarter Car Model. IEEE 1st Intern. Conf. on Power Electronics, Intelligent Control and Energy Systems (ICPEICES), Delhi, India, 4–6 July 2016. doi: 10.1109/ICPEICES.2016.7853369
- Ghaeminezhad N., Daobo W., Farooq F. Stabilizing a Gimbal Platform Using Self-Tuning Fuzzy PID Controller. International J. of Computer Applications. 2014, vol. 93, no.16, pp. 13–19.
- Seong K.-J., Kang H.-G., Yeo B.-Y., Lee H.-P. The Stabilization Loop Design for a Two-Axis Gimbal System Using LQG/LTR Controller. SICE-ICASE Intern. Joint Conf., Busan, South Korea, 18–21 Oct. 2006. doi: 10.1109/SICE.2006.315268

12. Baskin M., Leblebicioğlu M. K. Robust Control for Line-of-Sight Stabilization of a Two-Axis Gimbal System. Turkish J. of Electrical Engineering & Computer Sciences. 2017, vol. 25, no. 5, pp. 3839–3853.

13. Van Geffen V. A Study of Friction Models and Friction Compensation. Holland, Eindhoven: Technische Universiteit Eindhoven, 2009. 24 p.

14. Yang H., Zhao Y., Li M. Study on the Friction Torque Test and Identification Algorithm for Gimbal

Axis of an Inertial Stabilized Platform. Proc. of the Institution of Mechanical Engineers, Part G: J. of Aerospace Engineering. 2016, vol. 230, no. 10, pp. 1990–1999. doi: 10.1177/0954410015620709

15. Abdo M., Vali A. R., Toloei A. Research on the Cross-Coupling of a Two Axes Gimbal System with Dynamic Unbalance. Intern. J. of Advanced Robotic Systems. 2013, vol. 10, no. 10, p. 357. doi: 10.5772/56963

Information about the authors

Ngoc Hung Nguyen, Master in "Control and Automation Engineering" (2014), postgraduate student, lecturer at the Department of Aerospace Control Systems of Le Quy Don Technical University. The author of 3 scientific publications. Area of expertise: image processing for thermal camera; digital signal processing; control and estimation theory and intelligent controller designing.

Address: Le Quy Don Technical University, 236 Hoang Quoc Viet St., Bac Tu Liem, Ha Noi, Viet Nam

E-mail: hungnn@lqdtu.edu.vn

Van Phan Do, PhD (Eng.) (2014), lecturer at the Department of Aerospace Control Systems of Le Quy Don Technical University. The author of 3 scientific publications. Area of expertise: control and automation; navigation and control; smart control and combined control.

Address: Le Quy Don Technical University, 236 Hoang Quoc Viet St., Bac Tu Liem, Ha Noi, Viet Nam

E-mail: dovanphanhv@gmail.com

Hoa Tien Vu, PhD (Eng.) (2005), Associate Professor (2014), specialist in systems engineering control and automation, visiting lecturer at the Department of Aerospace Control Systems of Le Quy Don Technical University. The author of 53 scientific works and 4 scientific publications. Area of expertise: systems automatic control for UAV; electronic technology; systems engineering.

Address: Le Quy Don Technical University, 236 Hoang Quoc Viet St., Bac Tu Liem, Ha Noi, Viet Nam

E-mail: hoatien57@yahoo.com
